Memory-Event-Triggered H_∞ Output Control of Neural Networks With Mixed Delays

Shen Yan, Zhou Gu, *Member, IEEE*, and Sing Kiong Nguang, *Senior Member, IEEE*

***Abstract*—This article investigates the problem of memory-event-triggered H_∞ output feedback control for neural networks with mixed delays (discrete and distributed delays). The probability density of the communication delay among neurons is modeled as the kernel of the distributed delay. To reduce network communication burden, a novel memory-event-triggered scheme (METS) using the historical system output is introduced to choose which data should be sent to the controller. Based on a constructed Lyapunov–Krasovskii functional (LKF) with the distributed delay kernel and a generalized integral inequality, new sufficient conditions are formed by linear matrix inequalities (LMIs) for designing an event-triggered H_∞ controller. Finally, experiments based on a computer and a real wireless network are executed to confirm the validity of the developed method.**

***Index Terms*—Distributed delay, event-triggered control, neural networks, time-delay systems.**

I. Introduction

OVER the past decades, a considerable effort has been devoted to neural networks due to their wide applications in computer vision, deep learning, image encryption, Chua's circuit [1]–[7], and the references therein. It is noted that these applications are mainly dependent on the dynamic behaviors of neural networks, such as stability, chaos, and oscillatory. For example, the synchronization issue of neural networks utilizing the chaotic features is usually applied in image encryption. To reach the synchronization of master and slave neural networks, a synchronization issue is converted into a control problem of an error system, where a controller is designed to drive the slave neural network to track the master neural network in [4]. In addition, when the performance and stability of neural networks are deteriorated by noises or disturbances, a controller is usually used to improve them. In practical systems, time-delay problem is often encountered, which has gained much attention and inspired many results, for example, stability analysis [8]–[10] and stabilization [11]. It is common that there exist communication delays in the implementation of neural networks in real environments, which can deteriorate the system performance even make the system unstable. Thus, the issue of stabilization for neural networks with time delays becomes an interesting and hot research topic to obtain a desired system performance or reduce the convergence time. A great deal of interesting results have been addressed for this problem in [12]–[14] and the references therein. Recently, as the development of digital communication networks, network-based neural networks are considered for control [15] and state estimation [16] problems. Han *et al.* [15] addressed the network-based H_∞ control for neural networks with distributed delay, data quantization, and packet dropouts. In [16], the issue of networked H_∞ state estimation is studied for neural networks subject to network constraints, including the network-induced delay.

In real networked systems, the bandwidth of communication channel is limited usually, which is not considered in the aforementioned works. Thus, event-triggered scheme (ETS) is investigated to save the limited network resources and has gained growing attention from many researchers [17]–[20]. The problem of robust event-triggered adaptive control for uncertain nonlinear systems is developed in [21], where the full state constraints, system uncertainties, and measurement errors are considered simultaneously. In [22], an ETS using the relative error among the present system state and the last triggered state is proposed to ensure the input-to-state stability of both linear and nonlinear systems. Inspired by this work, various event triggering conditions are reported, such as periodic ETS [23], switching ETS [24], and dynamic ETS [25]. Different from these results knowing the stabilization controller in advance, Yue *et al.* [26] proposed a codesign method for handling the event-triggered control of linear networked control systems with communication delay, where the parameters of ETS and controller gain are designed simultaneously. For neural networks, following the codesign idea presented in [26] and [27] studies the issue of decentralized H_∞ control under ETS and cyberattacks. To cast the codesign conditions into linear matrix inequalities (LMIs), Zha *et al.* [27] assumed the control matrix satisfying full column rank, which is also assumed in [15]. Ding *et al.* [28] developed a new switched control strategy to cope with the stabilization issue of neural networks under the switching ETS [24]. The event-triggered synchronization control of switched delayed neural networks

Manuscript received 16 September 2020; revised 25 March 2021; accepted 22 May 2021. Date of publication 4 June 2021; date of current version 28 October 2022. This work was supported in part by the Natural Science Foundation of Jiangsu Province of China under Grant BK20200769, in part by the Natural Science Foundation of Jiangsu Provincial Universities under Grant 20KJB510045, and in part by the National Natural Science Foundation of China under Grant 61473156, Grant 61773200, and Grant 52005266. *(Corresponding author: Zhou Gu.)*

Shen Yan and Zhou Gu are with the College of Mechanical and Electronic Engineering, Nanjing Forestry University, Nanjing 210037, China (e-mail: yanshenzdh@gmail.com; gzh1808@163.com).

Sing Kiong Nguang, deceased, was with the Department of Electrical, Computer and Software Engineering, The University of Auckland, Auckland 1142, New Zealand (e-mail: sk.nguang@auckland.ac.nz).

Color versions of one or more figures in this article are available at https://doi.org/10.1109/TNNLS.2021.3083898.

Digital Object Identifier 10.1109/TNNLS.2021.3083898

is addressed in [29]. By employing the mode-dependent average dwell time approach, Yan *et al.* [30] investigated the design of sliding mode controller for switched neural networks with ETS.

Notice that the works of [26]–[30] only utilize the instant system information to design the triggering conditions, where the continuous system dynamics over a finite-time interval is not considered. Different from these results, Zhang *et al.* [31] proposed a novel ETS using the accumulation error of the system state, which could be helpful to further save network resources. However, under such triggering condition, it is difficult for codesigning the triggering parameters and the controller gain. Mousavi *et al.* [32] studied an integral-based ETS based on the average value of historical system state to attenuate the effect on control performance induced by stochastic measurement noise. In [32], the integral term induced by the triggering condition is treated via an approximation approach, which will result in the approximation error. In addition, the controller design methods in [27], [30], [32] are feasible only when all system states are available. Unfortunately, this requirement on the system state is hard to be realized in many practical applications [33], particularly for relatively large-scale neural networks [34], [35]. For neural networks with discrete and distributed delays, a few results about the event-triggered H_∞ control with memory-event-triggered scheme (METS) and measurement output are investigated, which motivates the present work.

This article studies the design of H_∞ static output controller for neural networks with discrete and distributed delays under the METS. A practical wireless network is built up to verify the effectiveness of the proposed ETS. We summarize the main contributions as follows.

1) A new METS utilizing the mean of measurement output is proposed to release the overoccupation of limited network bandwidth, and a constant scalar is inserted into the triggering condition to exclude the Zeno behavior. Compared with the existing ETS in [20] and [36] using instant system output, the proposed METS has the potential to reduce some unnecessary transmissions induced by the stochastic fluctuation of system dynamics.
2) The communication delays among neurons are described as a distributed delay term with a kernel representing the probability density and the integral term caused by the proposed METS can be viewed as another distributed delay term. The above two distributed delay terms are utilized directly in the design of Lyapunov–Krasovskii functional (LKF). Then, a novel integral inequality is applied to handle the distributed delay terms and derive the stability conditions. Compared with the existing method [37] using Legendre polynomials to approximate the kernel, the approximation error is avoided and the decision variables are decreased by the proposed LKF method. Moreover, the design conservativeness caused by approximation error will be eliminated.
3) By a proposed separation approach based on the Finsler lemma, the rank constraints on control matrix in some existing results [15], [27] are not required anymore. Moreover, the controller gain solved by the conventional left- and right-multiplying technique in [20] is dependent on the inverse of Lyapunov variable, while this coupling is removed by our proposed approach. Then, sufficient conditions are established via LMIs, which ensures the uniform ultimate bounded stability of the neural networks with prescribed H_∞ performance.

Notation: In this article, $\|\cdot\|$ is the Euclidean norm in $\mathbb{R}^n$. The transpose of a vector or matrix is denoted by the superscript "T." $X^\perp$ represents the kernel of X. $\mathrm{He}(X)$ equals $X^T + X$. The notation $\binom{k}{j}$ means the binomial coefficients given by $(k!/((k-j)!j!))$. $\otimes$ refers to the Kronecker product.

II. Preliminaries

Consider a complex dynamic system modeled by the following delayed neural networks:

$$\begin{cases} \dot{x}(t) = Ax(t) + N_0\psi(x(t)) + N_1\psi(x(t-\tau)) \\ \qquad + N_2\displaystyle\int_{t-\tau}^{t} g(\upsilon)\psi(x(\upsilon))d\upsilon + Bu(t) + D_1\omega(t) \\ y(t) = C_1x(t) \\ z(t) = C_2x(t) + D_2\omega(t) \end{cases} \tag{1}$$

where $x(t) = \mathrm{col}\{x_1(t), x_2(t), \ldots, x_n(t)\} \in \mathbb{R}^n$ is the state vector, $y(t) \in \mathbb{R}^r$ is the system output, $\psi(x(t)) = \mathrm{col}\{\psi_1(x_1(t)), \psi_2(x_2(t)), \ldots, \psi_n(x_n(t))\} \in \mathbb{R}^n$ denotes the neuron activation function, $u(t) \in \mathbb{R}^m$ is the control input, $\omega(t) \in \mathbb{R}^p$ satisfying $\omega(t) \in \mathcal{L}_2[0, \infty)$ is the external disturbance, $z(t) \in \mathbb{R}^q$ is the controlled output, the constant scalar τ denotes the discrete and distributed delays, and A, N_0, N_1, N_2, B, C_1, C_2, D_1, and D_2 are known real matrices and compatible with others. The pairs (A, B) and (A, C_1) are assumed to be controllable and detectable, respectively. The kernel of the distributed delay $g(\upsilon)$ is used to represent the probability density function of communication delay among neurons, which satisfies $\int_{-\tau}^{0} g(\upsilon)d\upsilon = 1$ and the following assumption.

Assumption 1: For the kernel $g(\upsilon)$ of the distributed delay term $\int_{-\tau}^{0} g(\upsilon)\psi(x(t+\upsilon))d\upsilon$, there exists a vector $\mathbf{g}(\upsilon) = [\, g_0(\upsilon) \cdots g_i(\upsilon) \cdots g_\alpha(\upsilon)\,]^T$, $g_0(\upsilon) \triangleq g(\upsilon)$, $i = 0, 1, \ldots, \alpha$ with $\alpha \in \mathbb{N}$ and $\upsilon \in [-\tau, 0]$ satisfying

$$\frac{d\mathbf{g}(\upsilon)}{d\upsilon} = \mathfrak{G}\mathbf{g}(\upsilon) \tag{2}$$

where $g_i(\upsilon)$ are linear independent, $\int_{-\tau}^{0} \mathbf{g}(\upsilon)\mathbf{g}^T(\upsilon)d\upsilon > 0$, and $\mathfrak{G} \in \mathbb{R}^{\alpha\times\alpha}$.

The neural activation function $\psi(\cdot)$ is usually nonlinear, which is difficult to be treated in stability analysis and synthesis. To deal with such difficulty with the same assumption in [29], the neural activation function $\psi(\cdot)$ is supposed to meet the following condition:

$$(\psi(x) - \mathscr{L}_1x)^T(\psi(x) - \mathscr{L}_2x) \le 0 \tag{3}$$

where $\mathscr{L}_1$ and $\mathscr{L}_2$ are two real constant matrices and satisfy $\mathscr{L}_2 - \mathscr{L}_1 \ge 0$.

Since the network bandwidth is limited, unnecessary data transmission will lead to a waste of the network communication resources. In order to decrease communication frequency, an METS is presented as

$$s_{k+1} = \min_{s} \ \{s \geq s_k | e^T(s)\Phi e(s) \geq \delta \hat{y}(s_k)^T \Phi \hat{y}(s_k) + \sigma\} \tag{4}$$

where $\delta \in (0,\ 1)$ is the triggering threshold parameter, $\sigma > 0$, $e(s) = (1/h)\int_{s-h}^{s} y(\upsilon)d\upsilon - \hat{y}(s_k)$, $\hat{y}(s_k) = (1/h)\int_{s_k-h}^{s_k} y(\upsilon)d\upsilon$, $y(s)$ is the current system output, $\hat{y}(s_k)$ and $\hat{y}(s_{k+1})$ mean the last and next triggered data, respectively, h is the integration time interval, and Φ is the positive weighting matrix.

Remark 1: The state and measured output of systems are highly possible to be inserted with some stochastic fluctuations caused by disturbances or noises in real-world applications. However, most existing ETSs [26]–[30] rely on instantaneous measured output, which are sensitive to such fluctuations and may trigger a lot of unnecessary signals. In order to adapt this scenario and increase the robustness of ETS against stochastic fluctuations, the average output over a given time interval h is introduced to construct the METS (4), which is more practical and has the potential to suppress such random fluctuations. Then, the data transmission is reduced and more network bandwidth can be saved than the conventional ETSs.

Remark 2: To exclude the Zeno phenomenon (infinite triggering events in finite period) in continuous-time ETS, a positive term σ is added in the METS by the similar way in [20]. With the help of this term, a positive lower bound of the interevent time can be obtained even though $\hat{y}(s_k) = 0$, which guarantees no Zeno behavior.

Remark 3: As $h \to 0$, $e(s) = (1/h)\int_{s-h}^{s} y(\upsilon)d\upsilon - \hat{y}(s_k)$ becomes $e(s) = y(s) - y(s_k)$. Then, the triggering condition (4) is reduced to

$$s_{k+1} = \min_{s} \ \{s > s_k | e^T(s)\Phi e(s) \geq \delta y(s_k)^T \Phi y(s_k) + \sigma\} \tag{5}$$

which is the existing ETS in [20] with $\Phi = I$ and [36] with $\sigma = 0$.

Denote the overall network communication delay from event generator to controller by a constant scalar h_1, which satisfies

$$t_k = s_k + h_1 < s_{k+1} + h_1 = t_{k+1}, \quad k \in \mathbb{N}. \tag{6}$$

Then, considering the network communication delay and zero-order holder (ZOH), the triggering condition (4) implies that

$$\epsilon^T(t)\Phi\epsilon(t) < \delta(\hat{y}(s_k))^T \Phi \hat{y}(s_k) + \sigma, \quad t \in [t_k,\ t_{k+1}) \tag{7}$$

where $\epsilon(t) \triangleq (1/h)\int_{t-h_2}^{t-h_1} y(\upsilon)d\upsilon - \hat{y}(s_k)$, $h_2 = h_1 + h$.

According to the above analysis, the static output controller is described as

$$u(t) = K\hat{y}(s_k) = KC_1\hat{x}(s_k), \quad t \in [t_k,\ t_{k+1}) \tag{8}$$

where the controller gain K needs to be designed later.

Therefore, substituting (8) and $\epsilon(t)$ defined in (7) into (1), the closed-loop system described by a system with distributed input delay is given as

$$\begin{cases} \dot{x}(t) = Ax(t) + N_0\psi(x(t)) + N_1\psi(x(t-\tau)) \\ \qquad + N_2\mathscr{I}_1\int_{-\tau}^{0}\mathscr{G}(\upsilon)\psi(x(t+\upsilon))d\upsilon - BK\epsilon(t) \\ \qquad + BKC_1\mathscr{I}_2\int_{t-h_2}^{t-h_1}\mathscr{F}(\upsilon)x(\upsilon)d\upsilon + D_1\omega(t) \\ z(t) = C_2x(t) + D_2\omega(t) \end{cases} \tag{9}$$

where

$$\begin{aligned} \mathscr{G}(\upsilon) &\triangleq \mathbf{g}(\upsilon) \otimes I_n, \quad g_0(\upsilon) = g(\upsilon) \\ \mathbf{g}(\upsilon) &= [g_0(\upsilon), \ldots, g_{\alpha_1}(\upsilon)]^T \\ \mathscr{F}(\upsilon) &\triangleq \mathbf{f}(\upsilon) \otimes I_n, \quad f_0(\upsilon) = 1/h \\ \mathbf{f}(\upsilon) &= [f_0(\upsilon), \ldots, f_{\alpha_2}(\upsilon)]^T. \end{aligned}$$

This article aims to obtain the static output feedback controller (8) such that the following conditions hold.

1) For $\omega(t) = 0$, the closed-loop system (9) is uniformly ultimately bounded.
2) For any $\omega(t) \neq 0$ and zero initial condition, the controlled output $z(t)$ satisfies

$$\int_0^\infty z^T(t)z(t)dt < \gamma^2\int_0^\infty \omega^T(t)\omega(t)dt \tag{10}$$

where γ represents the H_∞ index.

The following definition and technical lemmas are useful for obtaining the main results.

Definition 1 [20]: For the system (9) with $\omega(t) = 0$, if there exists a compact set $U \in \mathbb{R}^n$ such that for any $x(t_0 + \theta) = x_{t_0} \in U$, $\theta \in [-h_1,\ 0]$, there exists a $\sigma > 0$ and a number $\mathcal{T}(\sigma,\ x_{t_0})$ such that $\|x(t)\| < \sigma$, $\forall t \geq t_0 + \mathcal{T}$, the state of system (9) with $\omega(t) = 0$ is uniformly ultimately bounded.

Lemma 1 [38]: Given a positive symmetric matrix $\mathscr{U} \in \mathbb{R}^{n\times n}$ and a vector $\mathbf{g}(\upsilon)$ satisfying (2) in Assumption 1, one has

$$\int_{\eta_1}^{\eta_2} x^T(\upsilon)\mathscr{U}x(\upsilon)d\upsilon \geq [*](\mathscr{W} \otimes \mathscr{U})\int_{\eta_1}^{\eta_2}\mathscr{G}(\upsilon)x(\upsilon)d\upsilon \tag{11}$$

with $\mathscr{W}^{-1} = \int_{\eta_1}^{\eta_2}\mathbf{g}(\upsilon)\mathbf{g}^T(\upsilon)d\upsilon > 0$ and $\mathscr{G}(\upsilon) = \mathbf{g}(\upsilon) \otimes I_n$.

Remark 4: If the components of vector $\mathbf{g}(\upsilon)$ are chosen as Legendre polynomials

$$\begin{aligned} g_i(\upsilon) &= \mathbb{L}_i\left(\frac{\eta_2 - \upsilon}{\eta_2 - \eta_1}\right) \\ &= (-1)^i\sum_{j=0}^{i}(-1)^j\binom{i}{j}\binom{i+j}{j}\left(\frac{\eta_2-\upsilon}{\eta_2-\eta_1}\right)^j \end{aligned}$$

with $\mathscr{W}^{-1} = \text{diag}\{\eta_2 - \eta_1, ((\eta_2-\eta_1)/3), \ldots, ((\eta_2-\eta_1)/(2\alpha+1))\}$ for $i = 0, \ldots, \alpha$, one can get that (11) holds. This implies that (11) in Lemma 1 covers the Bessel–Legendre inequality in [37] as a special case.

Remark 5: By applying the presented METS with weighting function, the closed-loop H_∞ output control system is established as a novel distributed delay system. The distributed delay term can be approached by Legendre polynomials [37], which could lead to approximation error and conservativeness. Thus, the problem of treating the distributed delay and eliminating the approximation error is difficult and challenge. To solve this problem, a novel integral inequality (11) in Lemma 1 rather than Bessel–Legendre inequality based on Legendre polynomials is adopted. Then, the distributed delay term with weighting function in (9) can be treated directly, which avoids the approximation error.

III. Main Results

Theorem 1 gives the sufficient conditions for guaranteeing the H_∞ stability of the system (9) under the METS (4). In terms of Theorem 1, the corresponding conditions for code-signing the output controller gain and triggering parameters are formed in Theorem 2.

Theorem 1: For given constants τ, h, h_1, μ, ν, and δ, under the METS (4) and controller (8), the system (9) is uniformly ultimately bounded with a prescribed H_∞ index γ if there exist symmetric matrices P_N, $\Phi > 0$, $Q_1 > 0$, $Q_2 > 0$, $Q_3 > 0$, $R_1 > 0$, $R_2 > 0$, and $R_3 > 0$ and matrices X_1 and X_2 such that

$$\hat{P}_N > 0 \tag{12}$$

$$\Xi + He(\mathscr{X}\mathscr{Y}) < 0 \tag{13}$$

where

$$\begin{aligned}
\hat{P}_N &= P_N + \mathrm{diag}\{0_n, \mathscr{W}_1 \otimes Q_1, \mathscr{W}_2 \otimes Q_2, \mathscr{W}_3 \otimes Q_3\}\\
\Xi &= \begin{bmatrix} \Xi_1 & \Xi_2 \\ \Xi_2^T & -I \end{bmatrix}, \quad \bar{\mathscr{L}} = \begin{bmatrix} \bar{\mathscr{L}}_1 & \bar{\mathscr{L}}_2 \\ \bar{\mathscr{L}}_2^T & I \end{bmatrix}\\
\bar{\mathscr{L}}_1 &= \frac{\mathscr{L}_1^T\mathscr{L}_2 + \mathscr{L}_2^T\mathscr{L}_1}{2}, \quad \bar{\mathscr{L}}_2 = \frac{\mathscr{L}_1^T + \mathscr{L}_2^T}{2}\\
\Xi_1 &= He(H^T P_N M) + \delta\mathcal{E}_1^T\Phi\mathcal{E}_1 - \nu\mathcal{E}_2^T\bar{\mathscr{L}}\mathcal{E}_2\\
&\quad + \mathrm{diag}\{0_n, \Xi_{12}, \Xi_{13}, \Xi_{14}, \Xi_{15}, \Xi_{16}, \Xi_{17}, \Xi_{18}, \Xi_{19},\\
&\qquad \Xi_{110}, \Xi_{111}\}\\
\Xi_2 &= [\,0_n \quad C_2 \quad 0_n \quad 0_n \quad 0_n \quad 0_{n,(\alpha_1+1)n} \quad 0_{n,(\alpha_2+1)n}\\
&\qquad 0_{n,(\alpha_3+1)n} \quad 0_{n,r} \quad D_2 \quad 0_{n,q}\,]\\
\mathcal{E}_1 &= [\,0_{r,n} \quad 0_{r,n} \quad 0_{r,n} \quad 0_{r,n} \quad 0_{r,n} \quad 0_{r,n}\\
&\qquad 0_{r,(\alpha_1+1)n} \quad C_1\mathscr{I}_2 \quad 0_{r,(\alpha_3+1)n} \quad -I_r \quad 0_{r,p}\,]\\
\mathcal{E}_2 &= \begin{bmatrix} 0_n & I_n & 0_n & 0_n & 0_n & 0_{n,(\alpha_1+1)n} & 0_{n,(\alpha_2+1)n} & 0_{n,(\alpha_3+1)n} & 0_{n,r} & 0_{n,p} \\ 0_n & 0_n & 0_n & 0_n & I_n & 0_{n,(\alpha_1+1)n} & 0_{n,(\alpha_2+1)n} & 0_{n,(\alpha_3+1)n} & 0_{n,r} & 0_{n,p} \end{bmatrix}\\
\Xi_{12} &= Q_1 + h_1R_1 + \sigma^{\frac{1}{3}}I, \quad \Xi_{13} = -Q_1 + Q_2 + hR_2\\
\Xi_{14} &= -Q_2, \quad \Xi_{15} = Q_3 + \tau R_3, \quad \Xi_{16} = -Q_3\\
\Xi_{17} &= -\mathscr{W}_1 \otimes R_1, \quad \Xi_{18} = -\mathscr{W}_2 \otimes R_2\\
\Xi_{19} &= -\mathscr{W}_3 \otimes R_3, \quad \Xi_{110} = -\Phi, \quad \Xi_{111} = -\gamma^2 I\\
\mathscr{X} &= \big[\, X_1^T \quad X_2^T \quad 0_n \quad 0 \quad 0_n \quad 0_{n,(\alpha_1+1)n} \quad 0_{n,(\alpha_2+1)n}\\
&\qquad 0_{n,(\alpha_3+1)n} \quad 0_{n,r} \quad 0_{n,p} \quad 0_{n,q}\,\big]^T\\
\mathscr{Y} &= [-I \quad A \quad 0_n \quad 0_n \quad N_0 \quad N_1 \quad 0_{n,(\alpha_1+1)n}\\
&\qquad BKC_1\mathscr{I}_2 \quad N_2\mathscr{I}_1 \quad -BK \quad D_1 \quad 0_{n,q}]\\
M &= [M_1 \quad M_2 \quad M_3 \quad M_4], \quad H = [H_1 \quad H_2 \quad H_3]\\
M_1 &= \begin{bmatrix} I_n & 0_n & 0_n \\ 0_{(\alpha_1+1)n,n} & \mathscr{F}(0) & -\mathscr{F}(-h_1) \\ 0_{(\alpha_2+1)n,n} & 0_{(\alpha_2+1)n,n} & \mathscr{F}(-h_1) \\ 0_{(\alpha_3+1)n,n} & 0_{(\alpha_3+1)n,n} & 0_{(\alpha_3+1)n,n} \end{bmatrix}\\
M_2 &= \begin{bmatrix} 0_n & 0_n & 0_n \\ 0_{(\alpha_1+1)n,n} & 0_{(\alpha_1+1)n,n} & 0_{(\alpha_1+1)n,n} \\ -\mathscr{F}(-h_2) & 0_{(\alpha_2+1)n,n} & 0_{(\alpha_2+1)n,n} \\ 0_{(\alpha_3+1)n,n} & \mathscr{G}(0) & -\mathscr{G}(-\tau) \end{bmatrix}\\
M_3 &= \begin{bmatrix} 0_{n,(\alpha_1+1)n)} & 0_{n,(\alpha_2+1)n)} \\ -\widehat{\mathfrak{F}} & 0_{(\alpha_1+1)n,(\alpha_2+1)n} \\ 0_{(\alpha_2+1)n,(\alpha_1+1)n} & -\widehat{\mathfrak{F}} \\ 0_{(\alpha_3+1)n,(\alpha_1+1)n} & 0_{(\alpha_3+1)n,(\alpha_2+1)n} \end{bmatrix}\\
M_4 &= \begin{bmatrix} 0_{n,(\alpha_3+1)n)} & 0_{n,r} & 0_{n,p} \\ 0_{(\alpha_1+1)n,(\alpha_3+1)n} & 0_{(\alpha_1+1)n,r} & 0_{(\alpha_1+1)n,p} \\ 0_{(\alpha_2+1)n,(\alpha_3+1)n} & 0_{(\alpha_2+1)n,r} & 0_{(\alpha_2+1)n,p} \\ -\widehat{\mathfrak{G}} & 0_{(\alpha_3+1)n,r} & 0_{(\alpha_3+1)n,p} \end{bmatrix}\\
H_1 &= \begin{bmatrix} 0_n & I_n & 0_{n,3n} \\ 0_{(\alpha_1+1)n,n} & 0_{(\alpha_1+1)n,n} & 0_{(\alpha_1+1)n,3n} \\ 0_{(\alpha_2+1)n,n} & 0_{(\alpha_2+1)n,n} & 0_{(\alpha_2+1)n,3n} \\ 0_{(\alpha_3+1)n,n} & 0_{(\alpha_3+1)n,n} & 0_{(\alpha_3+1)n,3n} \end{bmatrix}\\
H_2 &= \begin{bmatrix} 0_{n,(\alpha_1+1)n} & 0_{n,(\alpha_1+1)n} \\ I_{(\alpha_1+1)n} & 0_{(\alpha_1+1)n,(\alpha_1+1)n} \\ 0_{(\alpha_2+1)n,(\alpha_1+1)n} & I_{(\alpha_2+1)n} \\ 0_{(\alpha_3+1)n,(\alpha_1+1)n} & 0_{(\alpha_3+1)n,(\alpha_1+1)n} \end{bmatrix}\\
H_3 &= \begin{bmatrix} 0_{n,(\alpha_3+1)n} & 0_{n,r} & 0_{n,p} \\ 0_{(\alpha_1+1)n,(\alpha_3+1)n} & 0_{(\alpha_1+1)n,r} & 0_{(\alpha_1+1)n,p} \\ 0_{(\alpha_2+1)n,(\alpha_3+1)n} & 0_{(\alpha_2+1)n,r} & 0_{(\alpha_2+1)n,p} \\ I_{(\alpha_3+1)n} & 0_{(\alpha_3+1)n,r} & 0_{(\alpha_3+1)n,p} \end{bmatrix}.
\end{aligned}$$

Proof: First, we choose the following LKF:

$$V(t) = \sum_{i=1}^{4} V_i(t) \tag{14}$$

where

$$\begin{aligned}
V_1(t) &= \zeta^T(t)P_N\zeta(t), \quad \zeta^T(t) = [x^T(t)\ \Omega^T(x)\ \Gamma^T(x)\ \Psi^T(x)]\\
V_2(t) &= \int_{t-h_1}^{t} x^T(\upsilon)[Q_1 + (\upsilon - t + h_1)R_1]x(\upsilon)d\upsilon\\
V_3(t) &= \int_{t-h_2}^{t-h_1} x^T(\upsilon)[Q_2 + (\upsilon - t + h_2)R_2]x(\upsilon)d\upsilon\\
V_4(t) &= \int_{t-\tau}^{t} \psi^T(x(\upsilon))[Q_3 + (\upsilon - t + \tau)R_3]\psi(x(\upsilon))d\upsilon\\
\Omega(x) &= \int_{-h_1}^{0} \mathscr{F}(\upsilon)x(t+\upsilon)d\upsilon\\
\Gamma(x) &= \int_{-h_2}^{-h_1} \mathscr{F}(\upsilon)x(t+\upsilon)d\upsilon\\
\Psi(x) &= \int_{-\tau}^{0} \mathscr{G}(\upsilon)\psi(x(t+\upsilon))d\upsilon.
\end{aligned}$$

For the chosen LKF (14), by applying Lemma 1, it yields

$$\int_{t-h_1}^{t} x^T(\upsilon)Q_1x(\upsilon)d\upsilon \geq \Omega^T(x)(\mathscr{W}_1 \otimes Q_1)\Omega(x) \tag{15}$$

$$\int_{t-h_2}^{t-h_1} x^T(\upsilon)Q_2x(\upsilon)d\upsilon \geq \Gamma^T(x)(\mathscr{W}_2 \otimes Q_2)\Gamma(x) \tag{16}$$

$$\int_{t-\tau}^{t} \psi^T(x(\upsilon))Q_3\psi(x(\upsilon))d\upsilon \geq \Psi^T(x)(\mathscr{W}_3 \otimes Q_3)\Psi(x). \tag{17}$$

From (14) and (15), one has

$$\begin{aligned}
V(t) \geq\ & \zeta^T(t)\hat{P}_N\zeta(t)\\
&+ \int_{t-h_1}^{t} x^T(\upsilon)(\upsilon - t + h_1)R_1x(\upsilon)d\upsilon\\
&+ \int_{t-h_2}^{t-h_1} x^T(\upsilon)(\upsilon - t + h_2)R_2x(\upsilon)d\upsilon\\
&+ \int_{t-\tau}^{t} \psi^T(x(\upsilon))(\upsilon - t + \tau)R_3\psi(x(\upsilon))d\upsilon.
\end{aligned} \tag{18}$$

Therefore, the positiveness of $V(t)$ results from the conditions $S_1 > 0$, $R_1 > 0$, $S_2 > 0$, $R_2 > 0$, and $\hat{P}_N > 0$.

By defining $\vartheta^T(t) = [\dot{x}^T(t), x^T(t), x^T(t-h_1), x^T(t-h_2), \psi^T(x(t)), \psi^T(x(t-\tau)), \Omega^T(x), \Gamma^T(x), \Psi^T(x), \epsilon^T(t), \omega^T(t)]$, it leads to

$$\zeta(t) = M\vartheta(t), \quad \dot{\zeta}(t) = H\vartheta(t). \tag{19}$$

Then, $\dot{V}(t)$ is obtained as

$$\dot{V}_1(t) = 2\zeta^T(t)P_N\dot{\zeta}(t) = 2\vartheta^T(t)H^TP_NM\vartheta(t) \tag{20}$$

$$\begin{aligned}\dot{V}_2(t) &= x^T(t)(Q_1 + h_1R_1)x(t) - x^T(t-h_1)Q_1x(t-h_1)\\ &\quad - \int_{t-h_1}^{t} x^T(\upsilon)R_1x(\upsilon)d\upsilon\end{aligned} \tag{21}$$

$$\begin{aligned}\dot{V}_3(t) &= x^T(t-h_1)(Q_2 + hR_2)x(t-h_1) - x^T(t-h_2)\\ &\quad \times Q_2x(t-h_2) - \int_{t-h_2}^{t-h_1} x^T(\upsilon)R_2x(\upsilon)d\upsilon\end{aligned} \tag{22}$$

$$\begin{aligned}\dot{V}_4(t) &= \psi^T(x(t))(Q_3 + \tau R_3)\psi(x(t))\\ &\quad - \psi(x(t-\tau))Q_3\psi(x(t-\tau))\\ &\quad - \int_{t-\tau}^{t} \psi^T(x(\upsilon))R_3\psi(x(\upsilon))d\upsilon.\end{aligned} \tag{23}$$

From the definitions of $\Omega(x)$, $\Gamma(x)$, and $\Psi(x)$ in (14), their derivatives are computed as

$$\begin{aligned}\dot{\Omega}(x) &= \mathscr{F}(0)x(t) - \mathscr{F}(-h_1)x(t-h_1)\\ &\quad - \widehat{\mathfrak{F}}\int_{-h_1}^{0} \mathscr{F}(\upsilon)x(t+\upsilon)d\upsilon\end{aligned} \tag{24}$$

$$\begin{aligned}\dot{\Gamma}(x) &= \mathscr{F}(-h_1)x(t-h_1) - \mathscr{F}(-h_2)x(t-h_2)\\ &\quad - \widehat{\mathfrak{F}}\int_{-h_2}^{-h_1} \mathscr{F}(\upsilon)x(t+\upsilon)d\upsilon\end{aligned} \tag{25}$$

$$\begin{aligned}\dot{\Psi}(x) &= \mathscr{G}(0)x(t) - \mathscr{G}(-\tau)x(t-\tau)\\ &\quad - \widehat{\mathfrak{G}}\int_{-\tau}^{0} \mathscr{G}(\upsilon)\psi(x(t+\upsilon))d\upsilon\end{aligned} \tag{26}$$

where $\widehat{\mathfrak{G}} = \mathfrak{G} \otimes I_{(\alpha_1+1)n}$ and $\widehat{\mathfrak{F}} = \mathfrak{F} \otimes I_{(\alpha_2+1)n}$.

To ensure the H_∞ stability of the system (9) based on the triggering condition (6), the following condition should be satisfied:

$$\begin{aligned}&\dot{V}(t) + z^T(t)z(t) - \gamma^2\omega^T(t)\omega(t)\\ &\quad \le \sum_{i=1}^{4} \dot{V}_i(t) + z^T(t)z(t) - \gamma^2\omega^T(t)\omega(t)\\ &\qquad + \delta\vartheta^T(t)\mathcal{E}_1^T\Phi\mathcal{E}_1\vartheta(t) - \epsilon^T(t)\Phi\epsilon(t)\\ &\qquad + \sigma - \sigma^{\frac{1}{3}}x^T(t)x(t) + \sigma^{\frac{1}{3}}x^T(t)x(t) < 0.\end{aligned} \tag{27}$$

Applying Lemma 1 to handle the integral terms in $\dot{V}_i(t)$ leads to

$$-\int_{t-h_1}^{t} x^T(\upsilon)R_1\ x(\upsilon)d\upsilon \le -\Omega^T(x)(\mathscr{W}_1 \otimes R_1)\Omega(x) \tag{28}$$

$$-\int_{t-h_2}^{t-h_1} x^T(\upsilon)R_2\ x(\upsilon)d\upsilon \le -\Gamma^T(x)(\mathscr{W}_2 \otimes R_2)\Gamma(x) \tag{29}$$

$$-\int_{t-\tau}^{t} \psi^T(x(\upsilon))R_3\psi(x(\upsilon))d\upsilon \le -\Psi^T(x)(\mathscr{W}_3 \otimes R_3)\Psi(x). \tag{30}$$

On the other hand, from (3), it leads to

$$[x^T(t) \quad \psi^T(x(t))]\begin{bmatrix} \bar{\mathscr{L}}_1 & \bar{\mathscr{L}}_2 \\ \bar{\mathscr{L}}_2^T & I \end{bmatrix}\begin{bmatrix} x(t) \\ \psi(x(t)) \end{bmatrix} \le 0$$

which results in

$$-\nu\vartheta^T(t)\mathcal{E}_2^T\bar{\mathscr{L}}\mathcal{E}_2\vartheta(t) \ge 0 \tag{31}$$

for any $\nu > 0$.

Combining (28)–(30), (31) is further ensured by

$$\hat{\vartheta}^T(t)\Xi\hat{\vartheta}(t) + \sigma - \sigma^{\frac{1}{3}}x^T(t)x(t) < 0 \tag{32}$$

where $\hat{\vartheta}^T(t) = [\ \vartheta^T(t)\ z^T(t)\ ]$.

Based on $\mathscr{Y}\hat{\vartheta}(t) = 0$ and constructed $\mathscr{X}$, one gets

$$\hat{\vartheta}^T(t)(\Xi + He(\mathscr{X}\mathscr{Y}))\hat{\vartheta}(t) + \sigma - \sigma^{\frac{1}{3}}x^T(t)x(t) < 0. \tag{33}$$

When $\|x(t)\| \ge \sigma^{(1/3)}$, one can get $\sigma^{(2/3)} - x^T(t)x(t) \le 0$. Since the condition (13) guarantees $\Xi + He(\mathscr{X}\mathscr{Y}) < 0$, it is obtained that (33) is guaranteed, which further ensures

$$\dot{V}(t) + z^T(t)z(t) - \gamma^2\omega^T(t)\omega(t) < 0. \tag{34}$$

It is noted that the closed-loop system (9) with $\omega(t) = 0$ is uniformly ultimately bounded based on Definition 1. Integrating both sides of (34) over $[0,\ \infty]$ and with the zero initial condition, one has $\int_0^\infty z^T(t)z(t)dt < \gamma^2\int_0^\infty \omega^T(t)\omega(t)dt$. Considering Definition 1 in [20], the closed-loop system (9) is ensured to be uniformly ultimately bounded. ■

According to Theorem 1, the corresponding control synthesis conditions are provided in Theorem 2.

Theorem 2: For given constants τ, h, h_1, μ, ν, and δ, considering the METS (4), the system (9) is uniformly ultimately bounded with a prescribed H_∞ index γ if there exist symmetric matrices P_N, $\Phi > 0$, $Q_1 > 0$, $Q_2 > 0$, $Q_3 > 0$, $R_1 > 0$, $R_2 > 0$, and $R_3 > 0$ and matrices X_1, X_2, Z, and W such that (12) and

$$\begin{bmatrix} \hat{\Xi}_1 & \Xi_2 & \Xi_3 \\ \Xi_2^T & -I & 0 \\ \Xi_3^T & 0 & -\mu He(W) \end{bmatrix} + He(\hat{\mathscr{X}}\hat{\mathscr{Y}}) < 0 \tag{35}$$

where

$$\begin{aligned}\hat{\Xi}_1 &= He(H^TP_NM) + \delta\mathcal{E}_1^T\Phi\mathcal{E}_1 - \nu\mathcal{E}_2^T\bar{\mathscr{L}}\mathcal{E}_2\\ &\quad + \mathrm{diag}\{0_n, \Xi_{12}, \Xi_{13}, \Xi_{14}, \Xi_{15}, \Xi_{16}, \Xi_{17}, \Xi_{18},\\ &\qquad \Xi_{19}, \Xi_{110}, \Xi_{111}\}\\ \Xi_3^T &= [\Xi_{31} \quad \Xi_{32} \quad 0_{m,4n} \quad 0_{m,(\alpha_1+1)n} \quad \Xi_{33}\\ &\qquad 0_{m,(\alpha_3+1)n} \quad \Xi_{34} \quad 0_m]\\ \Xi_{31} &= (X_1B - BW)^T, \quad \Xi_{32} = (X_2B - BW)^T\\ \Xi_{33} &= (ZC_1\mathscr{I}_2)^T, \quad \Xi_{34} = -Z^T\\ \hat{\mathscr{X}} &= [\hat{\mathscr{X}}_1 \quad \hat{\mathscr{X}}_2], \quad \hat{\mathscr{Y}} = [\hat{\mathscr{Y}}_1 \quad \hat{\mathscr{Y}}_2 \quad \hat{\mathscr{Y}}_3]\\ \hat{\mathscr{X}}_1 &= \begin{bmatrix} I_n & 0_n & 0_{n,4n} & 0_{n,(\alpha_1+1)n} & 0_{n,(\alpha_2+1)n} \\ 0_n & I_n & 0_{n,4n} & 0_{n,(\alpha_1+1)n} & 0_{n,(\alpha_2+1)n} \end{bmatrix}\\ \hat{\mathscr{X}}_2 &= \begin{bmatrix} 0_{n,(\alpha_3+1)n} & 0_{n,r} & 0_{n,p} & 0_{n,q} & 0_{n,m} \\ 0_{n,(\alpha_3+1)n} & 0_{n,r} & 0_{n,p} & 0_{n,q} & 0_{n,m} \end{bmatrix}^T\\ \hat{\mathscr{Y}}_1 &= \begin{bmatrix} -X_1 & X_1A & 0_{n,2n} & X_1N_0 & X_1N_1 \\ -X_2 & X_2A & 0_{n,2n} & X_2N_0 & X_2N_1 \end{bmatrix}\\ \hat{\mathscr{Y}}_2 &= \begin{bmatrix} 0_{n,(\alpha_1+1)n} & BZC_1\mathscr{I}_2 & 0_{n,\alpha_2 n} & X_1N_2\mathscr{I}_1 \\ 0_{n,(\alpha_1+1)n} & BZC_1\mathscr{I}_2 & 0_{n,\alpha_2 n} & X_2N_2\mathscr{I}_1 \end{bmatrix}\end{aligned}$$

$$\hat{\mathscr{Y}}_3 = \begin{bmatrix} 0_{n,\alpha_3 n} & -BZ & X_1 D_1 & 0_{n,q} & 0_{n,m} \\ 0_{n,\alpha_3 n} & -BZ & X_2 D_1 & 0_{n,q} & 0_{n,m} \end{bmatrix}.$$

Moreover, the controller gain is obtained as $K = W^{-1}Z$.

Proof: The condition (13) in Theorem 1 can be rewritten as

$$\mathcal{H}^{\perp^T}(\Xi + He(\mathscr{X}\mathscr{Y}))\mathcal{H}^{\perp} < 0 \tag{36}$$

where

$$\mathcal{H}^{\perp} = \begin{bmatrix} \mathcal{H}_1^{\perp} \\ \mathcal{H}_2^{\perp} \end{bmatrix}, \quad \mathcal{R} = \begin{bmatrix} \Xi + He(\mathscr{X}\mathscr{Y}) & 0 \\ 0 & 0 \end{bmatrix}$$
$$\mathcal{H}_1^{\perp} = \text{diag}\{I, I, I, I, I, \underbrace{I, \ldots, I}_{\alpha_1+\alpha_2+\alpha_3+3}, I, I, I\}$$
$$\mathcal{H}_2^{\perp} = [0_{m,6n} \quad 0_{m,(\alpha_1+1)n} \quad KC_1\mathscr{I}_2 \quad 0_{m,(\alpha_3+1)n} \quad -K \quad 0_{m,p} \quad 0_{m,q}].$$

Based on the structure of $\mathcal{H}^{\perp}$, the matrix $\mathcal{H}$ satisfying $\mathcal{H}\mathcal{H}^{\perp} = 0$ is given as

$$\mathcal{H} = [0_{m,6n} \quad 0_{m,(\alpha_1+1)n} \quad KC_1\mathscr{I}_2 \quad 0_{m,(\alpha_3+1)n} \quad -K \quad 0_{m,p} \quad 0_{m,q} \quad -I_m]. \tag{37}$$

To deal with the nonlinear terms X_1BKC_1 and X_2BKC_1 in (36), the matrix $\mathcal{M}$ is constructed as

$$\mathcal{M} = [\mathcal{M}_1 \quad \mathcal{M}_2 \quad 0_{m,4n} \quad 0_{m,(\alpha_1+1)n} \quad 0_{m,(\alpha_2+1)n} \quad 0_{m,(\alpha_3+1)n} \quad 0_{m,r} \quad 0_{m,p} \quad 0_{m,q} \quad \mu W^T]^T \tag{38}$$

where

$$\mathcal{M}_1 = (BW - X_1B)^T, \quad \mathcal{M}_2 = (BW - X_2B)^T.$$

Then, by applying the well-known Finsler lemma in [39] to (36) with (37) and (38), it gives

$$\mathcal{R} + He(\mathcal{M}\mathcal{H}) < 0 \tag{39}$$

which is equivalent to (35). Thus, the proof is ended. ■

Remark 6: When we choose $C_1 = I$, the corresponding state feedback controller designing conditions can be derived from Theorem 2 directly. In such a state feedback case, our controller designing method for neural networks has no rank constraint on the control matrix B, while it is always required in some existing results [15], [27].

Remark 7: The obtained results based on LMI conditions in Theorem 2 can be solved by MATLAB toolbox directly. The computation complexity of Theorem 2 is mainly dependent on the amount of decision variables ($\aleph = (((1 + (\sum_{i=1}^{3}\alpha_i + 4)n)(\sum_{i=1}^{3}\alpha_i + 4)n)/2))$ in the Lyapunov variable P_N, where α_i $(i = 1, 2, 3)$ mean the degrees of the vectors $\mathbf{g}(v)$ and $\mathbf{f}(v)$ and n is the number of the state variable. As the growth of α_i, computation complexity is increasing. However, less conservative results can be derived with higher computation complexity, which is shown in the following example.

TABLE I
DATA PACKET FORMAT

Name	Head	Function Port	Receiver Address	Data	End
Byte	2	2	2	variable	1

IV. EXAMPLE

Example 1: In this section, a cosimulation of a computer and a practical wireless network is implemented, shown in Fig. 1, where the system plant is carried out in computer and the control signals are propagated via the practical wireless network, which is connected with the computer via Arduino board. Some descriptions of the practical wireless network are given. The data packet transmitted via the ZigBee module is formed in Table I. In this experiment, the sampling period is 0.02 s and each control signal is represented by two bytes. If there are two control signals $\hat{y}_1(s_k)$ and $\hat{y}_2(s_k)$, the length of the data packet will be 11 bytes. The period of one transmission of the ZigBee module is 0.352 ms. According to the data sheet of the ZigBee module, the consumption energy of each transmission for one data packet is computed as 3.3 V × 30 mA × 0.352 ms = 0.034848 mJ, where 3.3 V is the operating voltage and 30 mA is the current during the transmission. From Fig. 1, one can see that the sender connected with the computer is used to send the triggered data to the network and receive the transmitted data from the network. Note that each data will be transmitted four times, that is, from the sender to the router, from the router to the receiver, from the receiver to the router, and from the router to the sender.

Then, the control issue of neural networks is applied to solve the synchronization problem of master–slave neural networks described as

$$\begin{cases} \dot{\theta}(t) = -A\theta(t) + N_0\phi(\theta(t)) + N_1\phi(\theta(t-\tau)) \\ \qquad + N_2\int_{-\tau}^{0} g(v)\phi(\theta(t+v))dv \\ \vartheta(t) = C_1\theta(t) \end{cases} \tag{40}$$

and

$$\begin{cases} \dot{\hat{\theta}}(t) = -A\hat{\theta}(t) + N_0\phi(\hat{\theta}(t)) + N_1\phi(\hat{\theta}(t-\tau)) \\ \qquad + N_2\int_{-\tau}^{0} g(v)\phi(\hat{\theta}(t+v))dv + Bu(t) + D_1\omega(t) \\ \hat{\vartheta}(t) = C_1\hat{\theta}(t). \end{cases} \tag{41}$$

By defining $x(t) = \hat{\theta}(t) - \theta(t)$, $y(t) = \hat{\vartheta}(t) - \vartheta(t)$, $\psi(x(t)) = \phi(\hat{\theta}(t)) - \phi(\theta(t))$, and $\psi(x(t-\tau)) = \phi(\hat{\theta}(t-\tau)) - \phi(\theta(t-\tau))$, the synchronization of systems (40) and (41) is transformed into the control system (1) with the following parameters:

$$A = \text{diag}\{-2, \ 0.2, \ -1, \ -3\}$$
$$B = \begin{bmatrix} 0.1 \\ 0.4 \\ 0.2 \\ 0.1 \end{bmatrix}, \quad N_0 = \begin{bmatrix} -0.1 & 1.1 & 0.2 & 0.3 \\ 0.1 & -0.1 & 0.2 & 0.2 \\ 0.3 & 0.8 & -0.5 & 1.2 \\ 0.4 & -0.1 & 1.3 & -0.4 \end{bmatrix}$$

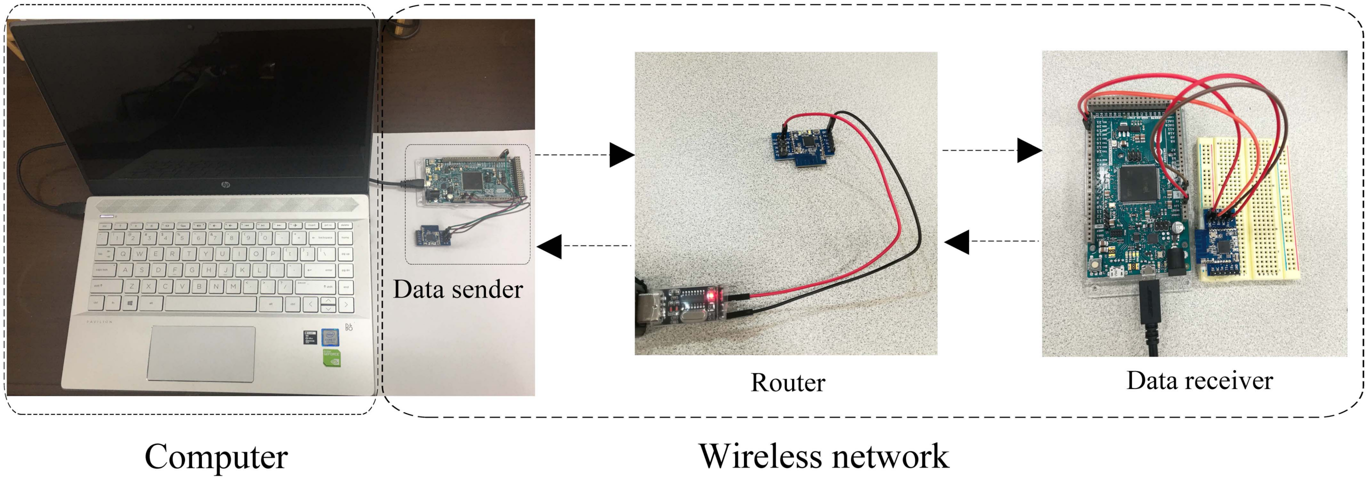

Fig. 1. Experiment setup.

$$N_1 = \begin{bmatrix} 0.1 & 0.2 & 0 & 0.5 \\ 0.2 & 0.1 & 0.2 & 0.2 \\ 0.4 & 0.2 & 0.2 & -0.1 \\ -0.3 & -0.1 & 0.2 & -0.3 \end{bmatrix}, \quad D_1 = \begin{bmatrix} 0.5 \\ 0.5 \\ 0.5 \\ 0.5 \end{bmatrix}$$
$$N_2 = \begin{bmatrix} -0.8 & 0.7 & 0.2 & 0.1 \\ -0.4 & -0.6 & 0.3 & -0.5 \\ 1.2 & -0.4 & -0.7 & -0.2 \\ 0.5 & -0.5 & 1.3 & -0.5 \end{bmatrix}, \quad D_2 = \begin{bmatrix} 0.1 \\ 0.1 \\ 0.1 \\ 0.1 \end{bmatrix}$$
$$C_1 = \begin{bmatrix} 1 & 0 & 0 & 1 \\ 0 & 1 & 1 & 1 \end{bmatrix}, \quad C_2 = I_4, \quad \psi_i(x_i) = \tanh(0.1x_i)$$
$$\mathscr{L}_1 = 0_4, \quad \mathscr{L}_2 = \mathrm{diag}\{0.1, 0.1, 0.1, 0.1\}.$$

As in [37] and [40], the probability density $g(\upsilon)$ of communication delays among neurons is usually approximated by a gamma distribution, which can be viewed as the distributed delay kernel. In this example, the upper bound of the communication delays is considered as $\tau = 0.25$, and then, the parameters of $g(\upsilon)$ are selected as $g(\upsilon) = -1230\upsilon e^{35\upsilon}$, $\upsilon \in [-\tau,\ 0]$ to satisfy the mathematic expression of gamma distribution and the feature of probability density $\int_{-\tau}^{0} g(\upsilon)d\upsilon = 1$. Based on $\dot{g}(\upsilon) = 35(-1230\upsilon e^{35\upsilon})+(-1230e^{35\upsilon})$ and Assumption 1 for $\alpha_i = 1$ $(i = 1, 2, 3)$, another term $-1230e^{35\upsilon}$ is added in $\mathbf{g}(\upsilon)$, which is given as

$$\mathbf{g}(\upsilon) = \begin{bmatrix} g_1(\upsilon) \\ g_2(\upsilon) \end{bmatrix} = \begin{bmatrix} -1230\upsilon e^{35\upsilon} \\ -1230e^{35\upsilon} \end{bmatrix}, \quad \mathfrak{G} = \begin{bmatrix} 35 & 1 \\ 0 & 35 \end{bmatrix}$$
$$\mathscr{G}(\upsilon) = \mathbf{g}(\upsilon) \otimes I_n, \quad \mathscr{I}_1 = [I_n \quad 0_{n,\alpha_1 n}]$$
$$\widehat{\mathfrak{G}} = \mathfrak{G} \otimes I_n, \quad \mathscr{W}_3^{-1} = \int_{-\tau}^{0} \mathbf{g}(\upsilon)\mathbf{g}^T(\upsilon)d\upsilon.$$

Following the similar way for $\mathbf{g}(\upsilon)$, we choose

$$\mathbf{f}(\upsilon) = \begin{bmatrix} f_1(\upsilon) \\ f_2(\upsilon) \end{bmatrix} = \begin{bmatrix} 1/h \\ \upsilon/h \end{bmatrix}, \quad \mathfrak{F} = \begin{bmatrix} 0 & 0 \\ 1 & 0 \end{bmatrix}$$
$$\mathscr{F}(\upsilon) = \mathbf{f}(\upsilon) \otimes I_n, \quad \widehat{\mathfrak{F}} = \mathfrak{F} \otimes I_n$$
$$\mathscr{W}_1^{-1} = \int_{-h_1}^{0} \mathbf{f}(\upsilon)\mathbf{f}^T(\upsilon)d\upsilon, \quad \mathscr{W}_2^{-1} = \int_{-h_2}^{-h_1} \mathbf{f}(\upsilon)\mathbf{f}^T(\upsilon)d\upsilon.$$

For $\tau = 0.25$, $h_1 = 0.04$, $h = 0.08$, $h_2 = h + h_1 = 0.12$, $\mu = 0.5$, $\nu = 20$, $\delta = 0.1$, and $\sigma = 10^{-6}$, the number of decision variables ($\aleph$) in P_N and the H_∞ performance γ computed by Theorem 2 for $\alpha_i = 1$ and $\alpha_i = 2$ $(i = 1, 2, 3)$ are derived in Table II. When $\alpha_i = 2$, the third terms of $\mathbf{g}(\upsilon)$ and $\mathbf{f}(\upsilon)$ are selected as $g_3(\upsilon) = -1230\upsilon^2 e^{35\upsilon}$ and $f_3(\upsilon) = \upsilon^2/h^2$, and the corresponding parameters can be obtained based on the same process of $\alpha_i = 1$, which are omitted here.

TABLE II
H_∞ PERFORMANCE γ FOR DIFFERENT VALUES OF α_i, $i = 1, 2, 3$

Theorem 2	$\alpha_i = 1$	$\alpha_i = 2$
γ	1.7125	0.6281
$\aleph$	448	880

It is observed from Table II that the H_∞ performance is improved as we increase α_1, α_2, and α_3. However, the larger α_1, α_2, and α_3 are chosen, and the more decision variables in matrix $\hat{P}_N$ will be used, which leads to higher computation burden and complexity. This illustrates that the proposed method has the potential to reduce the conservatism by increasing α_1, α_2, and α_3 at the cost of increasing computation complexity. The tradeoff between complexity and conservatism can be considered as: if the system performance is preferred to complex computation, one can increase the values of α_1, α_2, and α_3 to reduce conservatism. Otherwise, reduce these parameters to meet the required computational level.

The following simulations for the case $\alpha_1 = \alpha_2 = \alpha_3 = 1$ and case $\alpha_1 = \alpha_2 = \alpha_3 = 2$ are executed.

Based on Theorem 2 with $\alpha_1 = \alpha_2 = \alpha_3 = 1$, the corresponding controller gain K and triggering parameter Φ are obtained as

$$K = [-0.5569 \quad -1.7025], \quad \Phi = \begin{bmatrix} 1.5952 & 4.8693 \\ 4.8693 & 14.8859 \end{bmatrix}.$$

For $\alpha_1 = \alpha_2 = \alpha_3 = 2$, K and Φ are computed as

$$K = [1.5094 \quad -2.7679], \quad \Phi = \begin{bmatrix} 2.1921 & -3.9772 \\ -3.9772 & 7.2917 \end{bmatrix}.$$

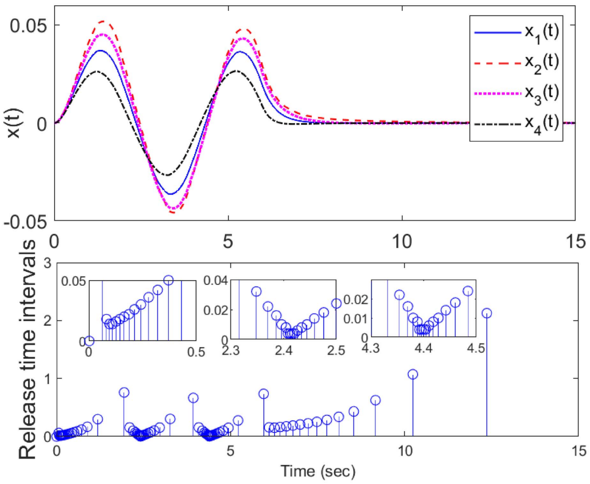

Fig. 2. State responses $x(t)$ and release instants for $\alpha_1 = \alpha_2 = \alpha_3 = 1$.

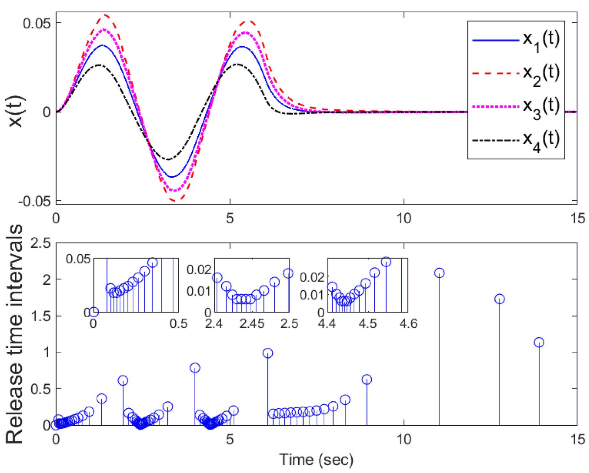

Fig. 3. State responses $x(t)$ and release instants for $\alpha_1 = \alpha_2 = \alpha_3 = 2$.

In the experiment, the considered master–salve type of neural networks is simulated in the computer and the proposed METS is also executed in it. The proposed METS is utilized to determine which signal should be transmitted to the controller. If a signal satisfies the triggering condition in METS, it will be triggered and send to the controller over the wireless network. Then, the triggered signal is used to control the slave system to track the master neural network. The exogenous disturbance is considered as $\omega(t) = \begin{cases} 2\sin(0.5\pi t), & 0 < t < 6 \text{ s} \\ 0, & \text{otherwise.} \end{cases}$ With the zero initial condition $x(0) = [0\ 0\ 0\ 0]^T$, sampling step 0.002 s, and the above parameters, the trajectories of state responses and release time intervals are shown in Fig. 2 for $\alpha_1 = \alpha_2 = \alpha_3 = 1$. The corresponding curves under $\alpha_1 = \alpha_2 = \alpha_3 = 2$ are shown in Fig. 3. According to these figures, it is obvious that the states of system are well stabilized when the external disturbance happens, which also implies that the neural networks (40) and (41) can be synchronized via the proposed METS control strategy.

TABLE III
NUMBER OF TRIGGERED EVENTS AND THE NETWORK ENERGY CONSUMPTION UNDER THE SAME $\gamma = 0.8$

ETS	$\mathscr{N}$	$\mathscr{E}(mJ)$
ETS in [36]	183	25.51
ETS in [20]	143	19.93
Our METS with $h = 0.01$	106	14.78
Our METS with $h = 0.03$	98	13.66
Our METS with $h = 0.07$	92	12.82

To show the effectiveness of the proposed METS for saving the precious communication resources, the stochastic disturbance $\omega(t) = 0.2\sin(0.5\pi t) + \beta(t)$ for $0 < t < 6$ s (otherwise, $\omega(t) = 0$) is considered, where $\beta(t)$ is a uniformly distributed random variable satisfying $|\beta(t)| \leq 1$. Choose $\sigma = 10^{-6}$ and the same H_∞ performance $\gamma = 0.8$. The comparison results of the amount of events generated by our METS with $\alpha_1 = \alpha_2 = \alpha_3 = 1$ and some existing ETSs are given in Table III, in which the energy values are computed by the formula $\mathscr{E} = \aleph \times 0.034848 \text{ mJ} \times 4$.

From Table III, one observes that the proposed METS (4) outperforms some existing ETSs on the energy consumed by wireless networks. Specially, compared to the existing ETS in [36] and ETS in [20], 49.74% and 35.47% energy can be saved by the proposed METS (4) with $h = 0.07$. This demonstrates the superiority of our proposed METS.

Remark 8: The proposed method is not specific to the master–slave type of neural networks. It can be applied to a class of artificial neural networks and the practical systems modeled by artificial neural networks satisfying the system model (1). For instance, the proposed method is applied to control a numerical artificial neural network and a Chua's circuit modeled by our presented system model in the next two examples.

Example 2: Choose the system (1) with the following parameters:

$$A = \begin{bmatrix} -0.4 & 0 \\ 0 & 0.2 \end{bmatrix},\ B = \begin{bmatrix} 0 \\ 1 \end{bmatrix},\ N_0 = \begin{bmatrix} -0.1 & 0.1 \\ 0.1 & -0.1 \end{bmatrix}$$
$$N_1 = \begin{bmatrix} -0.1 & 0.2 \\ 0.2 & -0.1 \end{bmatrix},\quad N_2 = \begin{bmatrix} -0.8 & 0.7 \\ -0.4 & -0.6 \end{bmatrix}$$
$$C_1 = \begin{bmatrix} 0.5 & 2 \\ 0 & 1 \end{bmatrix},\quad C_2 = I_2,\ D_1 = \begin{bmatrix} 0.2 \\ 0.1 \end{bmatrix},\ D_2 = \begin{bmatrix} 0.1 \\ 0.1 \end{bmatrix}$$
$$\psi_i(x_i) = \tanh(0.1x_i),\quad i = 1, 2.$$

$\psi(x)$ satisfies condition (3) with $\mathscr{L}_1 = 0_2$ and $\mathscr{L}_2 = \text{diag}\{0.1\ \ 0.1\}$.

Select $\tau = 0.25$, $h_1 = 0.04$, $h = 0.08$, $h_2 = h + h_1 = 0.12$, $\mu = 0.5$, $\nu = 20$, $\delta = 0.1$, $\sigma = 10^{-6}$, and $\alpha_1 = \alpha_2 = 1$.

In order to illustrate the advantage of the proposed method for dealing with the distributed delay term with kernel over the method based on Legendre polynomials in [37], the following comparisons are provided.

Moreover, Legendre polynomials given in the following are applied to approximate the kernel $g(v)$. For a chosen α_3,

TABLE IV
COMPARISON RESULTS OF $\aleph$ AND γ

Methods	$\aleph$	γ
Method in [37] with $\alpha_3 = 5$	264	0.5121
Method in [37] with $\alpha_3 = 4$	240	0.6551
Method in [37] with $\alpha_3 = 3$	180	0.6937
Method in [37] with $\alpha_3 = 2$	144	0.7143
Our method with $\alpha_3 = 2$	144	0.4524

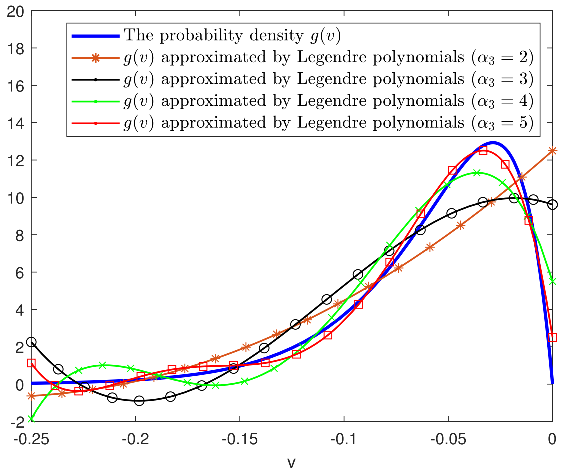

Fig. 4. $g(\upsilon)$ and $\hat{g}(\upsilon)$ with $\alpha_3 = 2, \ldots, 5$.

the approximated function $\hat{g}(\upsilon)$ is expressed as

$$\hat{g}(\upsilon) = \sum_{i=0}^{\alpha_3} \frac{2i+1}{\tau_M} \int_{-\tau_M}^{0} g(\upsilon)\mathbb{L}_i\left(\frac{-\upsilon}{\tau_M}\right)d\upsilon$$

where $\mathbb{L}_i(-\upsilon/\tau_M) = (-1)^i \sum_{j=0}^{i}(-1)^j \binom{i}{j}\binom{i+j}{j}(-\upsilon/\tau_M)^j$. The corresponding curves of the kernel $g(\upsilon)$ and the approximated function $\hat{g}(\upsilon)$ for different degrees are shown in Fig. 4. From Fig. 4, one observes that the larger α_3 is chosen, and the better performance of the approximation for $g(\upsilon)$ is obtained. As the increase of α_3, much more decision variables are needed by using Legendre polynomials. The amounts of decision variables ($\aleph$) in P_N and H_∞ performance γ with the Legendre polynomials and our presented approach are derived in Table IV. From this table, it is seen that both $\aleph$ and γ obtained by our method are smaller than the values obtained by the method in [37]. These illustrate that our method handling the kernel $g(\upsilon)$ without approximation error is less conservative than the one based on Legendre polynomials.

Example 3: In this example, we show that the considered system (1) can model some practical systems by choosing appropriate parameters. One of them is Chua's circuit, which is borrowed from [41] and modeled as

$$\begin{cases} \dot{x}_1(t) = -am_1x_1(t) + ax_2(t) - a(m_0 - m_1)\lambda(x_1(t)) \\ \dot{x}_2(t) = x_1(t) - x_2(t) + x_3(t) \\ \dot{x}_3(t) = -bx_2(t) \\ y(t) = x_1(t) \end{cases} \tag{42}$$

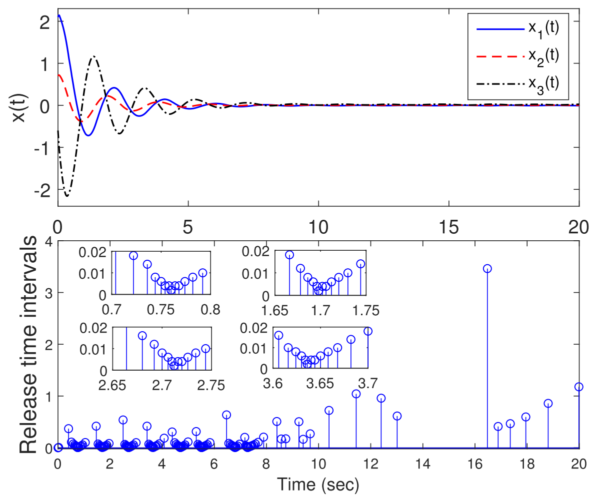

Fig. 5. Trajectories of the state and release instants.

TABLE V
$\aleph$ FOR DIFFERENT VALUES OF δ

δ	0.1	0.2	0.3
$\aleph$	198	181	159

with $a = 9$, $b = 14.28$, $c = 0.1$, $m_0 = -(1/7)$, and $m_1 = 2/7$ and the nonlinearities of Chua's diode

$$\lambda(x_1(t)) = 0.5(m_1 - m_0)(|x_1(t) + 1| - |x_1(t) - 1|).$$

Then, without considering the discrete and distributed delays and the disturbance, the closed-loop system of Chua's circuit can be transformed into the system (1) with

$$A = \begin{bmatrix} -\frac{18}{7} & 9 & 0 \\ 1 & -1 & 1 \\ 0 & -14.28 & 0 \end{bmatrix}, \quad N_0 = \begin{bmatrix} \frac{27}{7} \\ 0 \\ 0 \end{bmatrix}$$
$$C_1 = [1 \quad 0 \quad 0]$$
$$\psi(x_1(t)) = \lambda(x_1(t)), \quad L_0 = 1, \ L_2 = 1$$
$$N_1 = N_2 = 0, \quad B = I_3, \ \omega(t) = 0.$$

By selecting $h_1 = 0.02$, $h = 0.04$, $h_2 = h + h_1 = 0.06$, $\mu = 1$, $\nu = 10$, $\delta = 0.1$, $\sigma = 10^{-6}$, and $\alpha_1 = \alpha_2 = \alpha_3 = 1$, the controller gain and triggering matrix are solved as

$$K = [-1.6458 \quad -0.5361 \quad 2.0769]^T, \quad \Phi = 39.6878.$$

In the simulation, based on the same experiment setup in Example 1 and choosing the initial condition $x(0) = [2.1 \ 0.7 \ -0.6^T]$, the state response trajectories and release time intervals are given in Fig. 5. From this figure, one can see that the synchronization error system state of Chua's circuit can be stabilized well by our proposed memory-event-triggered control approach.

In addition, the number of triggering events under different values of δ is given in Table V. From this table, one can see that a larger value of σ is chosen, and fewer events will be triggered. On the contrary, a smaller σ will result in more triggering events.

V. Conclusion

This article focuses on the memory-event-triggered H_∞ output control issue of neural networks with discrete and distributed delays. A novel METS utilizing the mean of system output is presented to reduce the signal communication frequency. Compared with some existing ETMs based on instant system information, the proposed METS can decrease more data transmission. By using the Finsler lemma, a decomposition method is employed to extract the controller gain from system matrices and introduced variables. Resorting to a novel integral inequality technique, sufficient synthesis conditions for designing the event-triggered H_∞ static output controller are obtained via LMIs. Some cosimulations are executed to confirm the validity of the developed approach.

Acknowledgment

The authors would like to show their great gratitude to Prof. Sing Kiong Nguang for his contribution to this manuscript. Unfortunately, Prof. Nguang passed away in the middle of this work in 7th June 2020. He was a Distinguished Professor with the Department of Electrical, Computer and Software Engineering, The University of Auckland, Auckland, New Zealand, with a passion for the research of control systems. He was honored with many awards and recognitions for both his teaching and research. This section was provided by the coauthors in memory of him.

References

[1] C. K. Ahn, P. Shi, and L. Wu, "Receding horizon stabilization and disturbance attenuation for neural networks with time-varying delay," *IEEE Trans. Cybern.*, vol. 45, no. 12, pp. 2680–2692, Dec. 2015.

[2] R. Saravanakumar, M. S. Ali, C. K. Ahn, H. R. Karimi, and P. Shi, "Stability of Markovian jump generalized neural networks with interval time-varying delays," *IEEE Trans. Neural Netw. Learn. Syst.*, vol. 28, no. 8, pp. 1840–1850, Aug. 2017.

[3] P. Shi, F. Li, L. Wu, and C.-C. Lim, "Neural network-based passive filtering for delayed neutral-type semi-Markovian jump systems," *IEEE Trans. Neural Netw. Learn. Syst.*, vol. 28, no. 9, pp. 2101–2114, Sep. 2017.

[4] S. Lakshmanan, M. Prakash, C. P. Lim, R. Rakkiyappan, P. Balasubramaniam, and S. Nahavandi, "Synchronization of an inertial neural network with time-varying delays and its application to secure communication," *IEEE Trans. Neural Netw. Learn. Syst.*, vol. 29, no. 1, pp. 195–207, Jan. 2018.

[5] G. Rajchakit, P. Chanthorn, M. Niezabitowski, R. Raja, D. Baleanu, and A. Pratap, "Impulsive effects on stability and passivity analysis of memristor-based fractional-order competitive neural networks," *Neurocomputing*, vol. 417, pp. 290–301, Dec. 2020.

[6] P. Chanthorn, G. Rajchakit, U. Humphries, P. Kaewmesri, R. Sriraman, and C. P. Lim, "A delay-dividing approach to robust stability of uncertain stochastic complex-valued hopfield delayed neural networks," *Symmetry*, vol. 12, no. 5, p. 683, Apr. 2020.

[7] X. Yan, Y. Liu, Y. Xu, and M. Jia, "Multistep forecasting for diurnal wind speed based on hybrid deep learning model with improved singular spectrum decomposition," *Energy Convers. Manage.*, vol. 225, Dec. 2020, Art. no. 113456.

[8] Y. Wei, J. H. Park, H. R. Karimi, Y.-C. Tian, and H. Jung, "Improved stability and stabilization results for stochastic synchronization of continuous-time semi-Markovian jump neural networks with time-varying delay," *IEEE Trans. Neural Netw. Learn. Syst.*, vol. 29, no. 6, pp. 2488–2501, Jun. 2018.

[9] P. Chanthorn *et al.*, "Robust stability of complex-valued stochastic neural networks with time-varying delays and parameter uncertainties," *Mathematics*, vol. 8, no. 5, p. 742, May 2020.

[10] R. Sriraman, G. Rajchakit, C. P. Lim, P. Chanthorn, and R. Samidurai, "Discrete-time stochastic quaternion-valued neural networks with time delays: An asymptotic stability analysis," *Symmetry*, vol. 12, no. 6, p. 936, Jun. 2020.

[11] G. Rajchakit, A. Pratap, R. Raja, J. Cao, J. Alzabut, and C. Huang, "Hybrid control scheme for projective lag synchronization of Riemann–Liouville sense fractional order memristive BAM neural networks with mixed delays," *Mathematics*, vol. 7, no. 8, p. 759, Aug. 2019.

[12] L.-B. Wu, J. H. Park, X.-P. Xie, and Y.-J. Liu, "Neural network adaptive tracking control of uncertain MIMO nonlinear systems with output constraints and event-triggered inputs," *IEEE Trans. Neural Netw. Learn. Syst.*, vol. 32, no. 2, pp. 695–707, Feb. 2021.

[13] S. Yan, S. K. Nguang, and Z. Gu, "H_∞ weighted integral event-triggered synchronization of neural networks with mixed delays," *IEEE Trans. Ind. Informat.*, vol. 17, no. 4, pp. 2365–2375, Apr. 2021.

[14] V. N. Phat and H. Trinh, "Exponential stabilization of neural networks with various activation functions and mixed time-varying delays," *IEEE Trans. Neural Netw.*, vol. 21, no. 7, pp. 1180–1184, Jul. 2010.

[15] Q. L. Han, Y. Liu, and F. Yang, "Optimal communication network-based H_∞ quantized control with packet dropouts for a class of discrete-time neural networks with distributed time delay," *IEEE Trans. Neural Netw. Learn. Syst.*, vol. 27, no. 2, pp. 426–434, Feb. 2016.

[16] T. H. Lee, J. H. Park, and H. Jung, "Network-based H_∞ state estimation for neural networks using imperfect measurement," *Appl. Math. Comput.*, vol. 316, pp. 205–214, Jan. 2018.

[17] Z. Gu, C. K. Ahn, D. Yue, and X. Xie, "Event-triggered H_∞ filtering for T–S fuzzy-model-based nonlinear networked systems with multi-sensors against DoS attacks," *IEEE Trans. Cybern.*, early access, Nov. 5, 2020, doi: 10.1109/TCYB.2020.3030028.

[18] Q. Li, B. Shen, Z. Wang, and W. Sheng, "Recursive distributed filtering over sensor networks on Gilbert–Elliott channels: A dynamic event-triggered approach," *Automatica*, vol. 113, Mar. 2020, Art. no. 108681.

[19] Y. Liu, B. Shen, and H. Shu, "Finite-time resilient H_∞ state estimation for discrete-time delayed neural networks under dynamic event-triggered mechanism," *Neural Netw.*, vol. 121, pp. 356–365, Jan. 2020.

[20] C. Peng and Q.-L. Han, "Output-based event-triggered H_∞ control for sampled-data control systems with nonuniform sampling," in *Proc. Amer. Control Conf.*, Washington, DC, USA, Jun. 2013, pp. 1727–1732.

[21] H. Pan, X. Chang, and D. Zhang, "Event-triggered adaptive control for uncertain constrained nonlinear systems with its application," *IEEE Trans. Ind. Informat.*, vol. 16, no. 6, pp. 3818–3827, Jun. 2020.

[22] P. Tabuada, "Event-triggered real-time scheduling of stabilizing control tasks," *IEEE Trans. Autom. Control*, vol. 52, no. 9, pp. 1680–1685, Sep. 2007.

[23] W. P. M. H. Heemels and M. C. F. Donkers, "Model-based periodic event-triggered control for linear systems," *Automatica*, vol. 49, no. 3, pp. 698–711, Mar. 2013.

[24] A. Selivanov and E. Fridman, "Event-triggered H_∞ control: A switching approach," *IEEE Trans. Autom. Control*, vol. 61, pp. 3221–3226, 2016.

[25] A. Girard, "Dynamic triggering mechanisms for event-triggered control," *IEEE Trans. Autom. Control*, vol. 60, no. 7, pp. 1992–1997, Jul. 2015.

[26] D. Yue, E. Tian, and Q.-L. Han, "A delay system method for designing event-triggered controllers of networked control systems," *IEEE Trans. Autom. Control*, vol. 58, no. 2, pp. 475–481, Feb. 2013.

[27] L. Zha, E. Tian, X. Xie, Z. Gu, and J. Cao, "Decentralized event-triggered H_∞ control for neural networks subject to cyber-attacks," *Inf. Sci.*, vols. 457–458, pp. 141–155, Aug. 2018.

[28] S. Ding, Z. Wang, and H. Zhang, "Event-triggered stabilization of neural networks with time-varying switching gains and input saturation," *IEEE Trans. Neural Netw. Learn. Syst.*, vol. 29, no. 10, pp. 5045–5056, Oct. 2018.

[29] S. Wen, Z. Zeng, M. Z. Q. Chen, and T. Huang, "Synchronization of switched neural networks with communication delays via the event-triggered control," *IEEE Trans. Neural Netw. Learn. Syst.*, vol. 28, no. 10, pp. 2334–2343, Oct. 2017.

[30] H. Yan, H. Zhang, X. Zhan, Y. Wang, S. Chen, and F. Yang, "Event-triggered sliding mode control of switched neural networks with mode-dependent average dwell time," *IEEE Trans. Syst., Man, Cybern., Syst.*, vol. 51, no. 2, pp. 1233–1243, Feb. 2021.

[31] X.-M. Zhang, Q.-L. Han, and X. Yu, "Survey on recent advances in networked control systems," *IEEE Trans. Ind. Informat.*, vol. 12, no. 5, pp. 1740–1752, Oct. 2016.

[32] S. H. Mousavi and H. J. Marquez, "Integral-based event triggering controller design for stochastic LTI systems via convex optimisation," *Int. J. Control*, vol. 89, no. 7, pp. 1416–1427, Jul. 2016.

[33] S. Yan, Z. Gu, and C. K. Ahn, "Memory-event-triggered H_∞ filtering of unmanned surface vehicles with communication delays," *IEEE Trans. Circuits Syst. II, Exp. Briefs*, early access, Jan. 11, 2021, doi: 10.1109/TCSII.2021.3050760.
[34] P. Shi, Y. Zhang, and R. K. Agarwal, "Stochastic finite-time state estimation for discrete time-delay neural networks with Markovian jumps," *Neurocomputing*, vol. 151, pp. 168–174, Mar. 2015.
[35] H. Huang, T. Huang, X. Chen, and C. Qian, "Exponential stabilization of delayed recurrent neural networks: A state estimation based approach," *Neural Netw.*, vol. 48, pp. 153–157, Dec. 2013.
[36] S. Yan, M. Shen, W. Che, and G. Zhang, "Event-triggered non-fragile H_∞ filtering of linear systems with a structure separated approach," *IET Control Theory Appl.*, vol. 11, no. 17, pp. 2977–2984, Nov. 2017.
[37] A. Seuret, F. Gouaisbaut, and Y. Ariba, "Complete quadratic Lyapunov functionals for distributed delay systems," *Automatica*, vol. 62, pp. 168–176, Dec. 2015.
[38] Q. Feng and S. K. Nguang, "Stabilization of uncertain linear distributed delay systems with dissipativity constraints," *Syst. Control Lett.*, vol. 96, pp. 60–71, Oct. 2016.
[39] S. P. Boyd, L. E. Ghaoui, E. Feron, and V. Balakrishan, *Linear Matrix Inequalities in System and Control Theory*. Philadelphia, PA, USA: SIAM, 1994.
[40] O. Roesch and H. Roth, "Remote control of mechatronic systems over communication networks," in *Proc. IEEE Int. Conf. Mechatronics Autom.*, vol. 3, Niagara Falls, ON, Canada, Jun./Jul. 2005, pp. 1648–1653.
[41] S. Liu and L. Zhou, "Network synchronization and application of chaotic Lur'e systems based on event-triggered mechanism," *Nonlinear Dyn.*, vol. 83, no. 4, pp. 2497–2507, Mar. 2016.

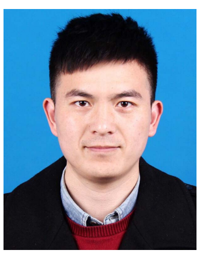

Shen Yan received the B.E. and Ph.D. degrees from the College of Electrical Engineering and Control Science, Nanjing Tech University, Nanjing, China, in 2014 and 2019, respectively.

From 2017 to 2018, he was a Visiting Ph.D. Student with The University of Auckland, Auckland, New Zealand. He is currently a Lecturer with the College of Mechanical and Electronic Engineering, Nanjing Forestry University, Nanjing. His current research interests include networked control systems, event-triggered control, and their applications.

Zhou Gu (Member, IEEE) received the B.S. degree from North China Electric Power University, Beijing, China, in 1997, and the M.S. and Ph.D. degrees in control science and engineering from the Nanjing University of Aeronautics and Astronautics, Nanjing, China, in 2007 and 2010, respectively.

From 1996 to 2013, he was with the School of Power Engineering, Nanjing Normal University, Nanjing, as an Associate Professor. He was a Visiting Scholar with Central Queensland University, Rockhampton, QLD, Australia, and The University of Manchester, Manchester, U.K. He is currently a Professor with Nanjing Forestry University, Nanjing. His current research interests include networked control systems, time-delay systems, reliable control, and their applications.

Sing Kiong Nguang (Senior Member, IEEE) received the B.E. (Hons.) and Ph.D. degrees from the Department of Electrical and Computer Engineering, The University of Newcastle, Callaghan, NSW, Australia.

He is currently a Chair Professor with the Department of Electrical, Computer and Software Engineering, The University of Auckland, Auckland, New Zealand. He has published over 300 refereed journal articles and conference papers on nonlinear control design, nonlinear control systems, nonlinear time-delay systems, nonlinear sampled-data systems, biomedical systems modeling, fuzzy modeling and control, biological systems modeling and control, and food and bioproduct processing.

Dr. Nguang has/had served on the editorial board for a number of international journals. He is the Editor-in-Chief of the *International Journal of Sensors, Wireless Communications and Control*.